sensors

MDPI

Article

A Dual-Polymer Fiber Fizeau Interferometer for Simultaneous Measurement of Relative Humidity and Temperature

Chao-Tsung Ma [1], Yu-Wei Chang [2], Yuan-Jie Yang [2] and Cheng-Ling Lee [2,*]

[1] Department of Electrical Engineering, National United University, Miaoli 36003, Taiwan; ctma@nuu.edu.tw
[2] Department of Electro-Optical Engineering, National United University, Miaoli 36003, Taiwan; as85635544@gmail.com (Y.-W.C.); nn4088nn40888@gmail.com (Y.-J.Y.)
* Correspondence: cherry@nuu.edu.tw; Tel.: +886-37-382568; Fax: +886-37-382555

Received: 19 October 2017; Accepted: 16 November 2017; Published: 17 November 2017

Abstract: This paper presents a novel design method in which a dual-polymer fiber Fizeau interferometer (DPFFI) is proposed for simultaneously measuring relative humidity (RH) and temperature (T). Since the polymer is intrinsically highly sensitive to both RH and T, the polymer fiber Fizeau interferometer (PFFI) exhibits cross-sensitivity of RH and T. In general, it is difficult to demodulate the optical responses from both variations of RH and T using a single PFFI. If two PFFIs with different structures are combined, they will individually exhibit distinct sensitivity responses with respect to RH and T, respectively. The technical problem of analyzing multiple interferences of the optical spectra of the DPFFI and the individual sensitivity of RH and T to each PFFI is obtained using the fast Fourier transform (FFT). A mathematical method is applied to solve the simultaneous equations of the DPFFI, so that the two variables RH and T can be determined at the same time. Experimental results, indicating good sensitivity and accuracy, with small measurement errors (average errors of ~1.46 °C and ~1.48%, respectively), are shown, determining the feasibility, and verifying the effectiveness, of the proposed DPFFI sensor.

Keywords: Fiber Fizeau interferometer (FFPI); polymer; fiber sensor; fast Fourier transform (FFT); simultaneously sensing humidity and temperature

1. Introduction

Relative humidity (RH) and temperature (T) are two significant physical parameters affecting a variety of industrial processes, such as semiconductor technology, food processing, biomedical engineering, weather forecasting, and environmental monitoring and control. In the above mentioned processes, the simultaneous measurement of RH and T provides a number of engineering advantages and is often a necessity for a variety of system applications. In recent years, several fiber optical sensors for simultaneous RH and T sensing have been proposed and investigated, but most of them are incorporated with well-known fiber devices such as fiber Bragg gratings (FBGs) [1–8], long-period fiber gratings (LPFGs) [8–10], and Fabry-Perot interferometers (FPIs) [1,11–13]. In [1], Arregui et al. proposed a sensor head composed of an FBG and a low-finesse FPI for simultaneous RH and T sensing. An RH measuring range from 11% to 97% RH and for T ranging from 10°C to 85 °C are shown. In their design case, the sensor head was connected to a single mode optical fiber network, which yielded a new possibility in multiplexing such sensors. An interesting fiber optic hybrid device composed of an FBG and a reflection-type photonic crystal fiber interferometer (PCFI) infiltrated with RH-sensitive agarose for simultaneous T and RH measurement was proposed and demonstrated in [2]. A measured T sensitivity of 9.8 pm/°C and an optical power variation of 7 dB upon a 75%RH change were shown. Another fiber device based on an FBG integrated with a photonic crystal fiber (PCF)-based in-fiber

Mach-Zehnder interferometer (MZI) was developed in [3], where a short PCF was fusion-spliced between two single-mode fibers and coated with a layer of a polyvinyl alcohol (PVA) material. With the RH measurement range up to 30–95% RH, the simultaneous measurement has been achieved with resolutions of 1 °C and 0.13% RH for T and RH, respectively. A knob-integrated FBG was proposed in [4]. By exciting the cladding modes as well as recoupling the reflected cladding modes back into the leading single mode fiber, the proposed sensor reached an RH sensitivity of up to 1.2 dB/% RH within an RH range of 30–95% and a T sensitivity of 8.2 pm/°C in the T range of 25–60 °C. Massaroni C. et al. proposed a configuration based on an array of FBGs for achieving the simultaneous measurement of both T and RH of gas in a chamber [5]. Another sensor consisting of a Fabry–Perot cavity formed by two identical FBGs was proposed in [6], where the polyimide material was coated on the FBG and also on the cavity with a different thickness. RH and T sensitivities of 1.92 pm/% RH and 8.87 pm/°C, respectively, with coating thicknesses of 10 μm on the FBG and 15 μm on the cavity, were shown. A hygroscopic polymer microcavity fiber Fizeau interferometer (PMFFI) incorporating a fiber Bragg grating (FBG) was proposed in [7] for the simultaneous measurement of RH and T. High sensitivity and accuracy were achieved. A long-period fiber grating (LPG)-based sensing head with an in-line FBG was proposed in [8] for simultaneous measurement of RH and T. Measured resolutions of 1.6% RH and 2.5 °C were achieved within an RH range from 20 to 50%, while 2.4% RH and 0.4 °C resolutions were achieved within an RH range from 50 to 80%. A fiber loop mirror sensor with a long period grating (LPG) inscribed in the polarization maintaining fiber (PMF) was proposed in [9]. RH and T sensitivities of 0.1723 nm/% RH and 0.2174 nm/°C with measurement errors of 2.6% RH and 0.2 °C, respectively, were demonstrated. The authors of [10] compared the differences between the RH and T sensing capabilities of fully and half-coated LPGs and reported a simple and cost-efficient method of measuring both T and RH, a possible alternative to cascaded LPGs sensing systems. The main contribution of the proposed dual-wavelength-based sensing method is the simultaneous measurement of RH and T using only one LPG. Results showed sensitivities of 63.23 pm/% RH and 410.66 pm/°C for the attenuation band corresponding to the coated contribution, and 55.22 pm/% RH and 405.09 pm/°C for the attenuation band corresponding to the uncoated grating. In 2014, a dielectric multilayer-based fiber optic sensor with simultaneous RH and T measurement capability was proposed in [11]. Average RH and T sensitivities of 0.43 nm/% RH and 0.63 nm/°C, respectively, when environmental RH changes from 1.8% RH to 74.7% RH and T changes from 21.4 to 38.8 °C, with high repeatability were shown. In [12], an all-silica miniature fiber-optic sensor based on two cascaded FPIs, formed at the tip of an optical fiber to measure T and RH, was proposed. The authors of [13] proposed a sensing device using an optical fiber Fabry-Perot interferometer. That sensor was constructed by splicing a short length of PCF to a single-mode fiber and coating an ultrathin PVA film onto the PCF's cleaved surface. However, of all the above-reviewed RH/T sensors, both the sensing sensitivity and resolution may not be high enough for certain high-tech applications. Furthermore, most of these fiber-grating-based sensors usually require complicated laser-written fabrication using expensive equipment.

In this work, simultaneous measurement of RH and T using a very simple and easily fabricated, dual-polymer fiber Fizeau interferometer (DPFFI) is presented. The polymer fiber Fizeau interferometer (PFFI) is based on a highly hygroscopic polymer directly coated on the end faces of two fibers. The presented hygroscopic polymer is highly sensitive to RH and T compared with previously reported fiber gratings. We strategically combined two PFFIs with different polymer lengths for the simultaneous measurement of RH and T. The key technical difficulty consisted in analyzing multiple interferences of optical spectra of the DPFFI and the individual RH and T sensitivities to each PFFI. By using the fast Fourier transform (FFT) and by solving a strategically simultaneous matrix inverse equation, the RH and T variables could be determined. Higher sensing sensitivities for RH and T were achieved, and no expensive equipment for laser-written fabrication of fiber-grating-based sensors was required. The proposed DPFFI device with design parameters of L_1 = 43.92 μm and L_2 = 12.5 μm was practically fabricated and tested under many different T/RH conditions. Experimental results

show that the proposed DPFFI sensor is capable of effectively and simultaneously measuring the surrounding RH and T with good accuracy.

2. Configuration and Sensing Principle

The hygroscopic polymer Norland optical adhesive 61 (NOA61) is a photo polymerizable monomer that can be made into a solid polymer by ultraviolet (UV) light curing. We have presented a polymer microcavity fiber Fizeau interferometer incorporating an FBG for simultaneously sensing RH and T [7]. Here in this design, the FBG is not required; however, two hygroscopic polymer fiber Fizeau interferometers (PFFIs) with different cavities are strategically combined to form the proposed DPFFI sensor for achieving the simultaneous measurement of T and RH, as shown in Figure 1. Figure 1 shows the layer of the proposed polymer acting as a cavity with two reflective interfaces R_1 and R_2, which reflects the optical signals back into the single mode fiber again so that reflection interference is achieved by the fiber Fizeau interferometer. By using monitored translation stages, the thick film of the polymer can be attached to the fiber end face and the UV-curing can be applied to form the first PFFI ($sensor_2$ in Figure 1). The coating and UV-curing steps can be repeated several times to obtain the second PPFI with a longer cavity length ($sensor_1$ in Figure 1). The optical characteristics of the coating polymer on SMF varies in response to the RH or T of the surrounding changes, affecting the optical length of the Fizeau cavity as well as the optical phase difference between the two reflected beams. According to the results in [7], this hygroscopic polymer was intrinsically highly sensitive to RH as well as T, and the RH/T sensitivities therein depended on the lengths of the polymer cavity. Thus, by combining two PPFIs with different responses of RH and T, respectively, the proposed sensor was able to individually extract the variations of RH and T from the surrounding area. Figure 2 displays the experimental setup for performing the simultaneous measurement. The light signal from a broad band light source propagates with a 2 × 2 coupler, reflects off the endfaces of $sensor_1$ and $sensor_2$, and returns to the coupler again. Finally, the combined spectral response readouts can be directly obtained by an optical spectrum analyzer (OSA).

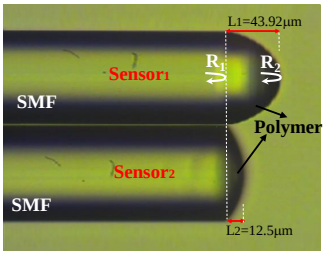

Figure 1. Configuration of the proposed dual-polymer fiber Fizeau interferometer (DPFFI) sensor.

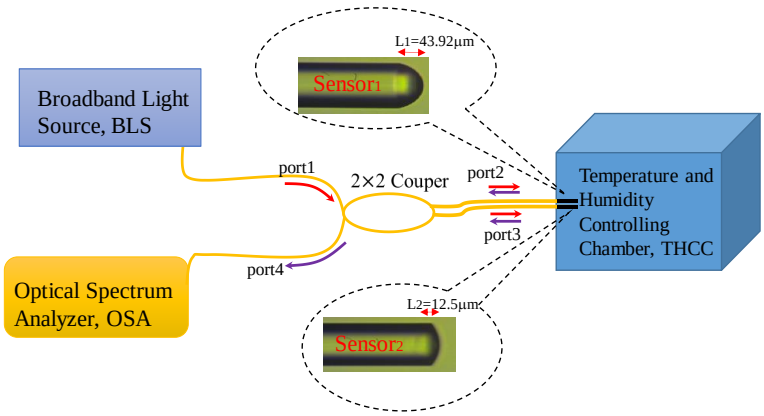

Figure 2. Experimental setup for simultaneously measuring RH and T.

Since we used two polymer sensors for the measurement of multiple parameters, the optical responses of the DPFFI are superimposed, will be displayed on the OSA. The analysis of the optical responses from the combined interferences can be accomplished using the fast Fourier transform (FFT) method. The FFT method was used to separate multiple interferences in spatial frequency into two individual spatial frequencies for sensor$_1$ and sensor$_2$, respectively. Figure 3 shows the processes of the optical response of the superimposed interference, separating into the spectra of interference$_1$ and interference$_2$ by the FFT method for sensor$_1$ and sensor$_2$, respectively. Figure 3a shows the multiple interferences of optical responses measured originally by the OSA. The spectral shifts are due to variations in the T and RH of the surrounding area, and the shifts that are caused by RH and/or T cannot be identified. Therefore, the signals of the superimposed interference of Figure 3a are processed by the FFT to obtain spatial frequency spectra, as shown in Figure 3b. We can then individually reconstruct interference$_1$ and interference$_2$ for sensor$_1$ and sensor$_2$ by the inverse fast Fourier transform (IFFT), as plotted in Figure 3c,d, respectively. Then, in an identical variation of T or RH, wavelength shifts of the optical interference$_1$ and interference$_2$ for sensor$_1$ and sensor$_2$ can be independently determined for achieving the simultaneous measurement of RH and T. In Figure 3c, the optical response of interference$_1$ can be inferred from the long-cavity of sensor$_1$ since high spatial frequency comes from the long-cavity in sensor$_1$. It can also be predicted that the sensitivities of RH and T in the long-cavity sensor$_1$ are smaller than those obtained by the short-cavity sensor$_2$.

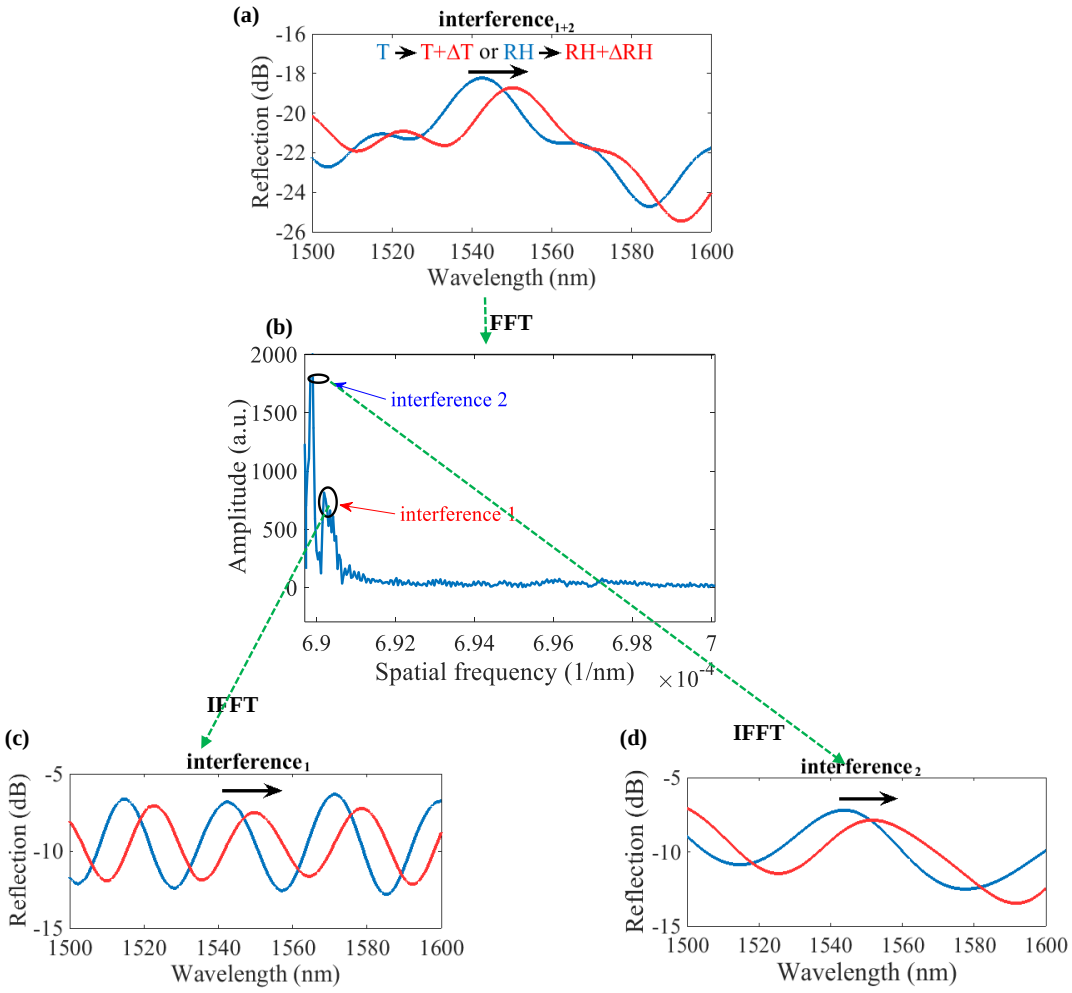

Figure 3. (**a**) Optical response of superimposed interference measured by the OSA; (**b**) superimposed spectra processed by FFT; separated optical spectra of (**c**) interference$_1$ and (**d**) interference$_2$, respectively.

If there are changes in temperature (ΔT) and relative humidity (ΔRH), wavelength shifts both from sensor$_1$ ($\Delta\lambda_1$) and sensor$_2$ ($\Delta\lambda_2$) can be respectively estimated using the simultaneous Equation (1a,b). In mathematics, a system of linear equations is a collection of two or more linear equations involving the same set of variables. Thus, a solution with several variables to a linear system can be obtained in which all the equations are simultaneously satisfied. Thus, by solving the simultaneous Equation (1a,b) of the sensing system, one can determine two variables (ΔT and ΔRH) at the same time.

$$\frac{\Delta\lambda_1}{\lambda_1} = \frac{1}{d_1}\frac{\partial d_1}{\partial T}\Delta T + B\Delta RH = A\Delta T + B\Delta RH. \tag{1a}$$

$$\frac{\Delta\lambda_2}{\lambda_2} = \frac{1}{d_2}\frac{\partial d_2}{\partial T}\Delta T + D\Delta RH = C\Delta T + D\Delta RH. \tag{1b}$$

In Equation (1a,b), A and C as well as B and D are the corresponding T and RH sensitivity coefficients for sensor$_1$ and sensor$_2$, respectively. Here, d_1 and d_2 denote the lengths of the polymer cavity for sensor$_1$ and sensor$_2$, respectively. The coefficients A, B, C, and D can be determined by measuring the individual spectral sensitivities of the two PFFIs in the DPFFI system with the variations in T and RH. Then, using the matrix inversion method, variations in temperature (ΔT) and relative humidity (ΔRH) can be simultaneously obtained by measuring the wavelength shifts of PFFI$_1$ ($\Delta\lambda_1$) and PFFI$_2$ ($\Delta\lambda_2$), respectively. The relation of the above parameters according to the Equation (1) is described below:

$$\begin{pmatrix} \Delta T \\ \\ \Delta RH \end{pmatrix} = \begin{pmatrix} A & B \\ C & D \end{pmatrix}^{-1} \begin{pmatrix} \frac{\Delta\lambda_1}{\lambda_1} \\ \\ \frac{\Delta\lambda_2}{\lambda_2} \end{pmatrix}. \tag{2}$$

Equation (2) can be simplified as follows:

$$\begin{pmatrix} \Delta T \\ \\ \Delta RH \end{pmatrix} = \begin{pmatrix} A' & B' \\ C' & D' \end{pmatrix}^{-1} \begin{pmatrix} \Delta\lambda_1 \\ \\ \Delta\lambda_2 \end{pmatrix} \tag{3}$$

where A', C', B' and D' represent the normalized coefficients for the T and RH sensitivities of sensor$_1$ and sensor$_2$, respectively. As a result, the sensitivity coefficients A', C', B', and D' in the sensing configuration need to be evaluated primarily to achieve the simultaneous measurement of RH and T.

3. Experimental Results and Discussion

In the experiment, the proposed DPFFI device was placed inside a temperature and humidity controlling chamber (THCC), as displayed in Figure 2, which was a closed space in which the T was increased from 20 to 50 °C and RH was fixed. The measured results are shown in Figure 4. The spectral responses to T are displayed in Figure 4a,c for sensor$_1$ and sensor$_2$, respectively. Based on the individual responses of interference$_1$ and interference$_2$ of sensor$_1$ and sensor$_2$, the T sensitivities of sensor$_1$ and sensor$_2$ to T are +0.25376 nm/°C and +0.39551 nm/°C, respectively, plotted in Figure 4b,d. Again, the device was placed in a condition where RH was increased from 20 to 90% and T was fixed at 25 °C. Figure 5 shows the RH sensitivities of sensor$_1$ and sensor$_2$: +0.12538 nm/%RH and +0.15807 nm/%RH, respectively. These results demonstrate that the proposed sensor has a wavelength redshift response when either T or RH is increased. It can also be inferred that shorter cavity lengths have larger free spectral ranges (FSRs) with greater T and RH sensitivities. However, it could be that, because of the possible overlap of interference dips, the measurement range is limited by the length of the FSR. The amount of wavelength shifts approaching the FSR will lead to the overlap of interference signals, so the wavelength shifts cannot be well identified. To avoid an overlap of interference dips, appropriate ranges of T (20~50 °C) and RH (20~90%) were considered in our study to obtain the T and RH sensitivity slopes and to demonstrate the proposed sensing method.

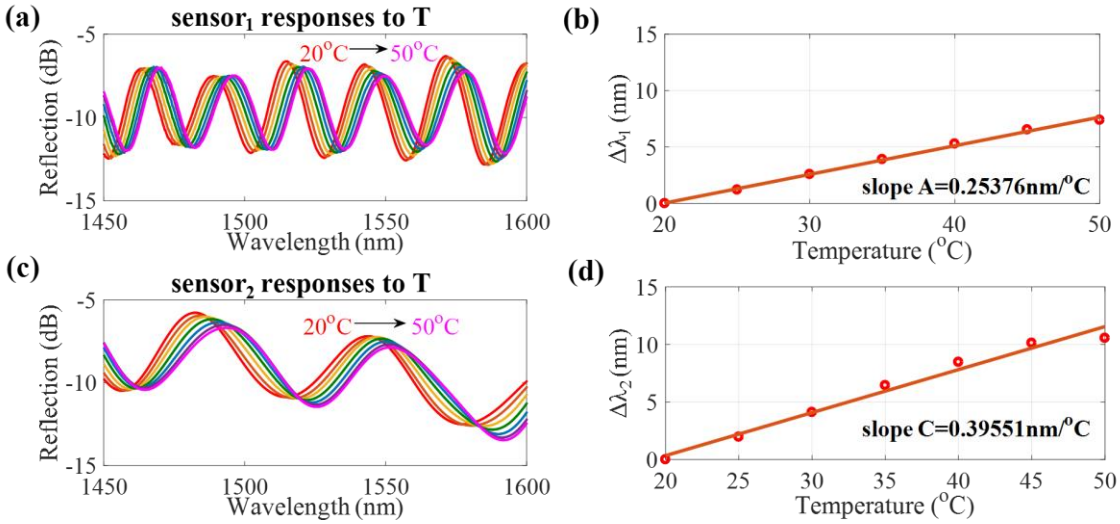

Figure 4. (**a**,**c**) Interference spectra of sensor$_1$ and sensor$_2$ for different T values, respectively; (**b**,**d**) Corresponding T sensitivities for sensor$_1$ and sensor$_2$, respectively.

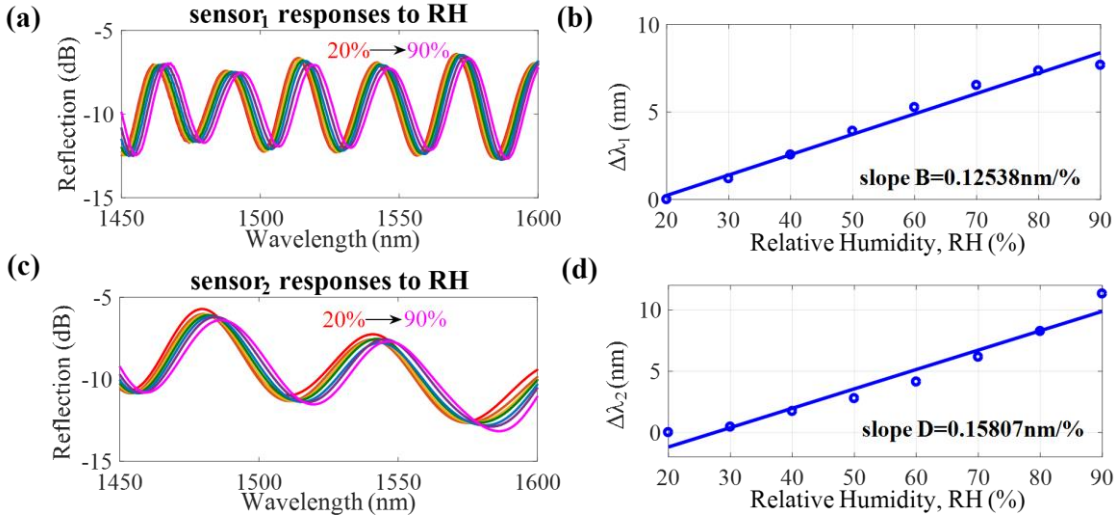

Figure 5. (**a**,**c**) Interference spectra of sensor$_1$ and sensor$_2$ for different RH values, respectively; (**b**,**d**) Corresponding RH sensitivities for sensor$_1$ and sensor$_2$, respectively.

Based on the above experimental results, the normalized sensitivity parameters A', B', C', and D' are the T and RH sensitivity coefficients of sensor$_1$ and sensor$_2$, which are estimated to be 0.25376 nm/°C, 0.12538 nm/%RH, 0.39551 nm/°C, and 0.15807 nm/%RH, respectively. The matrix inversion method is then utilized to perform the simultaneous measurement of RH and T. The analytical simultaneous equation, Equation (3), can be expressed as Equation (4). The inverse matrix can then be used to simplify Equation (4), yielding Equation (5).

$$\begin{pmatrix} \Delta T \\ \Delta RH \end{pmatrix} = \begin{pmatrix} A' & B' \\ C' & D' \end{pmatrix}^{-1} \begin{pmatrix} \Delta\lambda_1 \\ \Delta\lambda_2 \end{pmatrix} = \begin{pmatrix} 0.25376 & 0.12538 \\ 0.39551 & 0.15807 \end{pmatrix}^{-1} \begin{pmatrix} \Delta\lambda_1 \\ \Delta\lambda_2 \end{pmatrix}. \quad (4)$$

$$\begin{pmatrix} \Delta T \\ \Delta RH \end{pmatrix} = \frac{1}{-9.4914 \times 10^{-3}} \begin{pmatrix} 0.25376 & -0.39551 \\ -0.12538 & 0.15807 \end{pmatrix} \begin{pmatrix} \Delta\lambda_1 \\ \Delta\lambda_2 \end{pmatrix}. \quad (5)$$

To investigate the effectiveness of Equation (5) for the developed sensing configuration, T and RH were simultaneously varied from their reference values of ambient T_0 = 20 °C and RH_0 = 20% to conditions shown in Figures 6 and 7. The optical spectra of the initial condition of T_0 = 20 °C and RH_0 = 20% for $sensor_1$ and $sensor_2$ were recorded at the beginning of the experimental tests (The blue line in Figure 7). The Figure 6 presents the simultaneous measurement of random T and RH values under various levels. The blue circles represent the states of the T and RH levels in the temperature and humidity controlling chamber (THCC). The red triangles are the measured data evaluated by the proposed method. One can see that, in Figure 6, the simultaneous sensing of T and RH was accomplished. The average errors of the T and RH measurements in Figure 6 are about ~1.46 °C and ~1.48 %, respectively. We think that the errors are attributable to the measured deviations of the THCC machine and errors of numerical calculation. The results of three randomly selected cases—(a) T = 50 °C, RH = 40%, (b) T = 40 °C, RH = 65%, and (c) T = 55 °C, RH = 90% (marked in Figure 6)—whose measured spectral data and optical wavelength shifts are shown in Figure 7 and evaluated in Table 1, respectively.

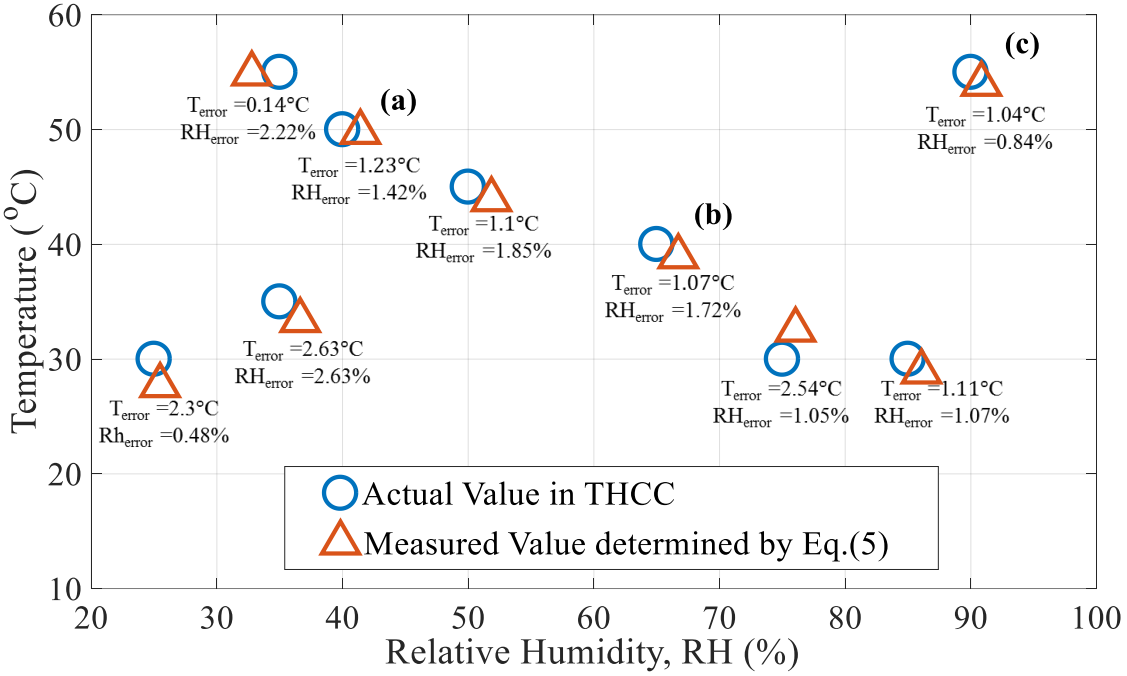

Figure 6. Sample data for measurement comparison.

In Condition (a) of Figure 7 as well as in Table 1, the measured wavelength shifts of $sensor_1$ and $sensor_2$ are $\Delta\lambda_1$= 10.24 nm and $\Delta\lambda_2$=15.16 nm, respectively. Based on Equation (5), the changes in T and RH are readily obtained as ΔT = +29.77 °C and ΔRH = +21.42%, respectively. Thus, the measurements of T and RH in the Condition (a) are T_m = 20 + 29.77 = 49.77 °C and RH_m = 20 + 21.42 = 41.42%, respectively. The simultaneously measured values of T_m and RH_m are very similar to the actual values displayed in the THCC. The errors in T and RH are 0.23 °C and 1.42%, respectively. The other two measurements of Conditions (b) and (c) with measured values of $\Delta\lambda_1$ = 10.66 nm and $\Delta\lambda_2$ = 14.87 nm, and $\Delta\lambda_1$ = 17.50 nm and $\Delta\lambda_2$ = 24.63 nm, used to determine T_m and RH_m, are also shown in Table 1 and Figure 7. The above evaluation demonstrates that effectiveness of the proposed DPFFI sensor.

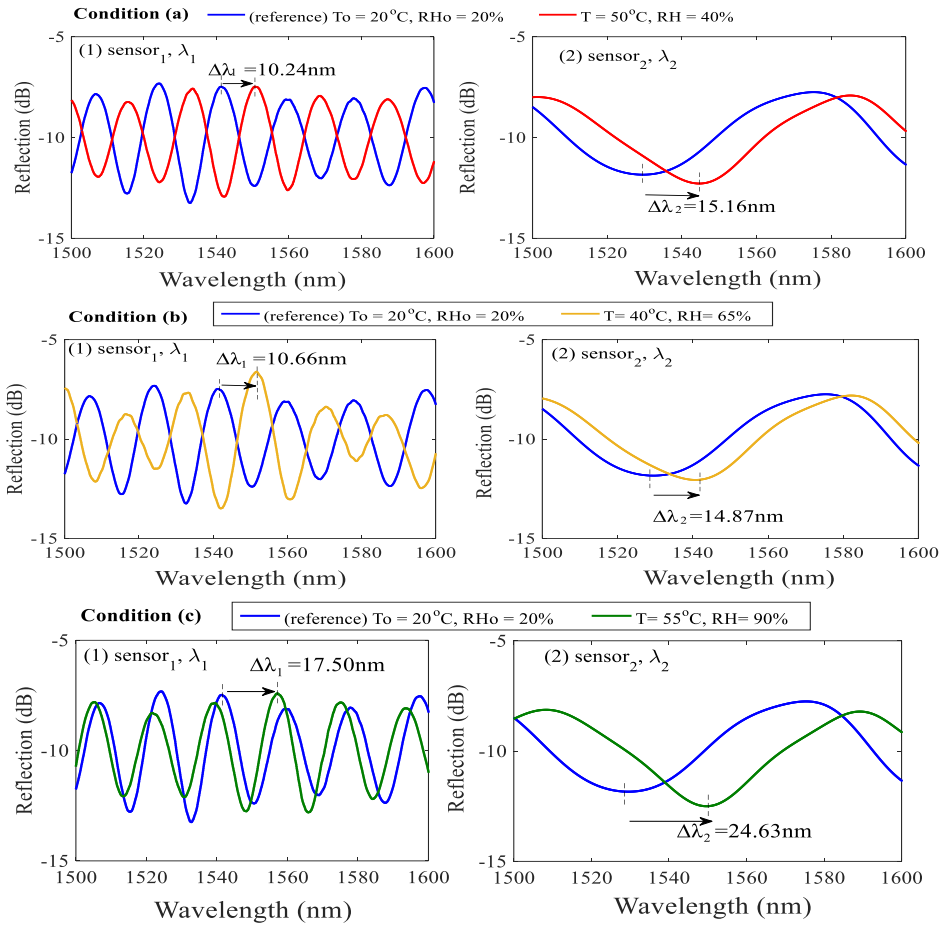

Figure 7. (1) and (2) are interference spectra shifts of sensor$_1$ and sensor$_2$, respectively, when RH and T change simultaneously in Conditions (**a**–**c**).

Table 1. Evaluating the simultaneous measurement of T and RH variations in different conditions of the proposed sensor.

Parameter / Condition	(a) T = 50 °C, RH = 40%	(b) T = 40 °C, RH = 65%	(c) T = 55 °C, RH = 90%
$\Delta\lambda_1$ (nm) $\Delta\lambda_2$ (nm)	+10.24 +15.16	+10.66 +14.87	+17.50 +24.63
Determined by Equation (5)	ΔT = + 29.77 °C ΔRH = + 21.42%	ΔT = +18.93 °C ΔRH = +46.72%	ΔT = +33.96 °C ΔRH = +70.84%
Measured T_m and RH_m	$T_m = T_0 + \Delta T$ = 49.77 °C $RH_m = RH_0 + \Delta RH$ = 41.42%	$T_m = T_0 + \Delta T$ = 38.93 °C $RH_m = RH_0 + \Delta RH$ = 66.72%	$T_m = T_0 + \Delta T$ = 53.96 °C $RH_m = RH_0 + \Delta RH$ = 90.84%
$T_{error} = \lvert T_m - T \rvert$ $RH_{error} = \lvert RH_m - RH \rvert$	T_{error} = 0.23 °C RH_{error} = 1.42%	T_{error} = 1.07 °C RH_{error} = 1.72%	T_{error} = 1.04 °C RH_{error} = 0.84%

4. Conclusions

We have developed a dual polymer fiber Fizeau interferometer (DPFFI) and used it to measure relative humidity (RH) and temperature (T) simultaneously using the fast Fourier transform (FFT) and a strategically mathematical matrix inversion relation. Since the proposed PFFI is highly sensitive to T and RH, sensing configuration of the developed DPFFI strategically combined with two different PFFIs can individually identify the variations in T and RH to achieve the objective of simultaneous measurement. The sensing principle is based on the fact that both PFFIs exhibit diverse RH and T sensitivities, respectively. Comprehensive experimental tests have been accomplished. Consistent

results show that, by using the proposed sensing scheme with a simple mathematical method, the proposed DPFFI can simultaneously and effectively measure T and RH with small errors in sensing ranges of T = 20~50 °C and RH = 20~90%.

Acknowledgments: The authors would like to thank the Ministry of Science and Technology of Taiwan, MOST 105-2221-E-239-01 and MOST 106-2221-E-239-014 to support the research.

Author Contributions: This work was carried out in collaboration between all authors. The first author Chao-Tsung Ma proposed the sensing concept, verified the mathematical method, analyzed the data, revised and polished the final manuscript. Authors, Yu-Wei Chang and Yuan-Jie Yang, the undergraduate students in the Department of EOE, performed the experiments, managed figures and data. The corresonding author, Cheng-Ling Lee, designed the experiments, verified the results and wrote the first draft of the manuscript.

Conflicts of Interest: The authors declare no conflict of interest.

References

1. Arregui, F.J.; Matías, I.R.; Cooper, K.L.; Claus, R.O. Simultaneous measurement of humidity and temperature by combining a reflective intensity-based optical fiber sensor and a fiber Bragg grating. *IEEE Sens.* **2002**, *2*, 482–487. [CrossRef]
2. Mathew, J.; Semenova, Y.; Farrell, G. Fiber optic hybrid device for simultaneous measurement of humidity and temperature. *IEEE Sens. J.* **2013**, *13*, 1632–1636. [CrossRef]
3. Zhang, S.Q.; Dong, X.Y.; Li, T.; Chan, C.C.; Shum, P.P. Simultaneous measurement of relative humidity and temperature with PCF-MZI cascaded by fiber Bragg grating. *Opt. Commun.* **2013**, *303*, 42–45. [CrossRef]
4. Yan, G.F.; Liang, Y.H.; Lee, E.-H.; He, S. Novel Knob-integrated fiber Bragg grating sensor with polyvinyl alcohol coating for simultaneous relative humidity and temperature measurement. *Opt. Express* **2015**, *23*, 15624–15634. [CrossRef] [PubMed]
5. Massaroni, C.; Caponero, M.A.; D'Amato, R.; Lo Presti, D.; Schena, E. Fiber Bragg grating measuring system for simultaneous monitoring of temperature and humidity in mechanical ventilation. *Sensors* **2017**, *17*, 749. [CrossRef] [PubMed]
6. Yulianti, I.; Supa'at, A.S.M.; Idrus, S.M.; Anwar, M.R.S. Design of fiber Bragg grating-based Fabry-Perot sensor for simultaneous measurement of humidity and temperature. *Optik* **2013**, *124*, 3919–3923. [CrossRef]
7. Lee, C.L.; You, Y.W.; Dai, J.H.; Hsu, J.M.; Horng, J.S. Hygroscopic polymer microcavity fiber Fizeau interferometer incorporating a fiber Bragg grating for simultaneously sensing humidity and temperature. *Sens. Actuators B Chem.* **2016**, *222*, 339–346. [CrossRef]
8. Viegas, D.; Hernaez, M.; Goicoechea, J.; Santos, J.L.; Araújo, F.M.; Arregui, F.; Matias, I.R. Simultaneous measurement of humidity and temperature based on an SiO_2-Nanospheres film deposited on a long-period grating in-line with a fiber Bragg grating. *IEEE Sens. J.* **2010**, *11*, 162–166. [CrossRef]
9. Liu, H.; Liang, H.; Sun, M.; Ni, K.; Jin, Y. Simultaneous measurement of humidity and temperature based on a long-period fiber grating inscribed in fiber loop mirror. *IEEE Sens. J.* **2013**, *14*, 893–896. [CrossRef]
10. Urrutiaa, A.; Goicoecheaa, J.; Ricchiutib, A.L.; Barrerab, D.; Salesb, S.; Arreguia, F.J. Simultaneous measurement of humidity and temperature based on a partially coated optical fiber long period grating. *Sens. Actuators B Chem.* **2016**, *227*, 135–141. [CrossRef]
11. Yang, M.; Xie, W.; Dai, Y.; Lee, D.; Dai, J.; Zhang, Y.; Zhuang, Z. Dielectric multilayer-based fiber optic sensor enabling simultaneous measurement of humidity and temperature. *Opt. Express* **2014**, *22*, 11892–11899. [CrossRef] [PubMed]
12. Pevec, S.; Donlagic, D. Miniature all-silica fiber-optic sensor for simultaneous measurement of relative humidity and temperature. *Opt. Lett.* **2015**, *40*, 5646–5649. [CrossRef] [PubMed]
13. Sun, H.; Zhang, X.L.; Yuan, L.T.; Zhou, L.B.; Qiao, X.G.; Hu, M.L. An Optical Fiber Fabry-Perot Interferometer Sensor for Simultaneous Measurement of Relative Humidity and Temperature. *IEEE Sens. J.* **2015**, *15*, 2891–2897. [CrossRef]